

Fig. 2 (left). Mercury close flyby geometry, viewed from the trajectory north pole. Fig. 3 (right). Mercury encounter as viewed from Earth, showing Earth occultation immersion and emersion.

(26-m antenna, 10-kw transmitter) and Goldstone DSS 14; DSS 12 had been maintaining uplink for command purposes in order that DSS 14 could be operated in a "listen only" mode to receive the high rate imaging. The 100-km DSS 14 transmitter was required to provide an adequate signal-to-noise ratio in the received spacecraft carrier and its superimposed range code. The forward beam of the infrared radiometer (IRR) intersected Mercury's surface at 2022 G.M.T., leaving at 2044 G.M.T. The IRR mode-2 command (aft beam, planet; forward beam, reference) was sent by the CC & S at that time; 1 minute later, the aft beam intersected the surface, continuing measurement until crossing the far limb at 2057 G.M.T.

Data obtained during passage through Earth occultation was recorded on the spacecraft tape recorder and played back several times starting at 16 hours after encounter. With the exception of this playback, the outgoing sequence mirrored the incoming one but was terminated after an imaging search for a Mercury satellite conducted at encounter plus 4 days.

After Mercury encounter operations, the spacecraft was returned to its cruise state for the long voyage around the sun and back to Mercury. A TCM was conducted on 9-10 May to allow a re-encounter with Mercury on 21 September 1974 between 2100 and 2200 G.M.T.

The scientific results obtained at Mercury are of significant planetological interest. The distinctly nonlunar solar wind interaction region characterized by the existence of a planetary magnetic field and structured streams

of accelerated electrons and protons is as exciting as it was unexpected. Whether that field is induced or intrinsic, its implications with respect to the internal constitution of the planet may be profound. The existence of extensive areas of terrain morphologically similar to the lunar mare material, combined with the planet's high density and the apparently primordial character of the surface in general, leads to important speculations concerning the nature of processes which occurred early in Mercury's history, the understanding of which may lead to modifications in theories dealing with the formation and subsequent evolution of the terrestrial planets. It should be remembered, however, that Mariner 10 has given us but a brief glimpse of Mercury, raising, as do most initial ven-

tures in planetary exploration, many more questions than it has answered. But the questions now have a sharper focus, and their answers a clearer place in the hierarchy of solar system studies.

JAMES A. DUNNE

Jet Propulsion Laboratory,
California Institute of Technology,
Pasadena 91103

References and Notes

1. J. A. Dunne, *Science* **183**, 1289 (1973). The Mariner 10 launch time which was reported to be 0245 on 2 November 1973 was in fact 0545 on 3 November.
2. R. C. Clauss and E. R. Wiebe, *Jet Propulsion Lab. Tech. Rep. 32-1516 XIX* (1974), p. 93.
3. I thank J. Y. Pedigo of the Jet Propulsion Laboratory (JPL) for assistance in the preparation of figures and manuscript and D. G. Rea and J. B. Jones of JPL for critical review and comment. This report represents one aspect of research carried out by JPL under NASA contract NAS 7-100.

31 May 1974

Preliminary Infrared Radiometry of the Night Side of Mercury from Mariner 10

Abstract. *The infrared radiometer on Mariner 10 measured the thermal emission from the planet with a spatial resolution element as small as 40 kilometers in a broad wavelength band centered at 45 micrometers. The minimum brightness temperature (near local midnight) in these near-equatorial scans was 100°K. Along the track observed, the temperature declined steadily from local sunset to near midnight, behaving as would be expected for a homogeneous, porous material with a thermal inertia of $0.0017 \text{ cal cm}^{-2} \text{ sec}^{-1/2} \text{ }^\circ\text{K}^{-1}$, a value only slightly larger than that of the moon. From near midnight to dawn, however, the temperature fluctuated over a range of about 10°K, implying the presence of regions having thermal inertia as high as $0.003 \text{ cal cm}^{-2} \text{ sec}^{-1/2} \text{ }^\circ\text{K}^{-1}$.*

The average thermophysical properties of the upper few centimeters of the Mercurian soil can be inferred from measurements of the cooling curve of the surface during the night. The night

temperatures are sensitive primarily to a single parameter, the thermal inertia $(K\rho c)^{1/2}$ of the soil (I), which in turn depends primarily on the porosity of the soil. Temperature fluctuations

around a mean cooling curve ("thermal anomalies") also provide a sensitive means of identifying inhomogeneities in the structure of surface materials due, for instance, to exposures of rock in an otherwise powdery surface. The infrared radiometer experiment on Mariner 10 was designed to measure the surface brightness temperature along a near-equatorial track from mid-afternoon across the night side to mid-morning, local time. In this preliminary report we will discuss only the data from the night side—19 hours to 05 hours, local time.

The radiometer is essentially the same as that flown on Mariners 6, 7, and 9 (2), but with modifications as necessary to accept radiation in the two spectral bands from approximately 8 to 14 μm and 35 to 55 μm . The radiometer was fixed relative to the spacecraft and gave two scans of Mercury, first by the "forward" beam, which traversed the evening side of the planet, and then by the "aft" beam, which traversed the morning side. The observations discussed in this report, falling as they do near the lower end of the temperature range of the radiometer, were all made with the long-wave (45- μm) channel. The field of view was 1.1°, providing a maximum linear resolution of 90 km for the forward beam and 40 km for the aft beam. At the minimum temperature measured, $\sim 100^\circ\text{K}$, the temperature resolution was limited by the digitization interval, which corresponded to $\Delta T \approx 0.5^\circ\text{K}$.

At the time of the flyby, Mercury was near aphelion and the longitude of the sunset terminator was 9°, where the origin of longitudes is the so-called "hot meridian," one of the two meridians that alternately face the sun at perihelion (3). The forward beam crossed the evening terminator at a latitude of -21° , swept gradually northward to achieve its highest linear resolution near 23 hours local time at a latitude of -12° , and left the planet near 02 hours local time.

The track of the aft beam was parallel to and slightly north of the forward beam, but close enough that there was substantial overlap in the surface areas observed between longitudes 310° and 250°. The highest resolution of the aft beam was near 250° (about local time 02 hours) and at latitude $+5^\circ$. The aft beam crossed the morning terminator at $+22^\circ$ latitude. At the time of this writing, final trajectory information has not been

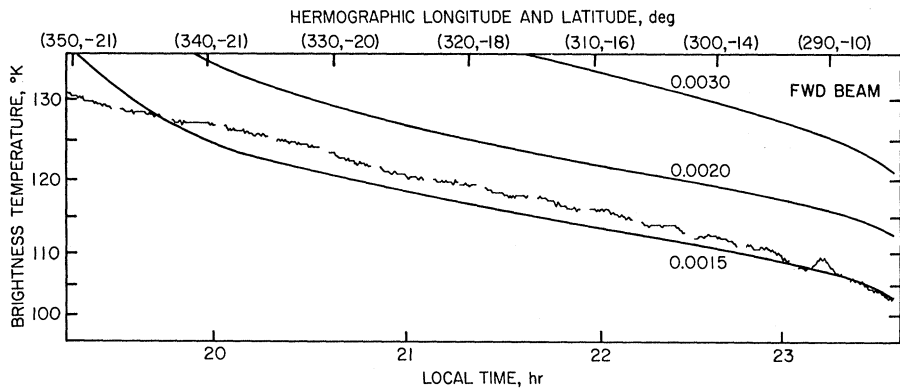


Fig. 1 (top) Brightness temperatures of Mercury at 45 μm obtained from the trace of the forward beam. The plot is linear in 45- μm intensity and in spacecraft time. The ordinate is labeled in brightness temperature and the abscissa in local time and in hermographic longitude and latitude. Three model curves, as described in the text, are labeled by their thermal inertias. The data gaps are due to 6.0 seconds of calibration each 42 seconds.

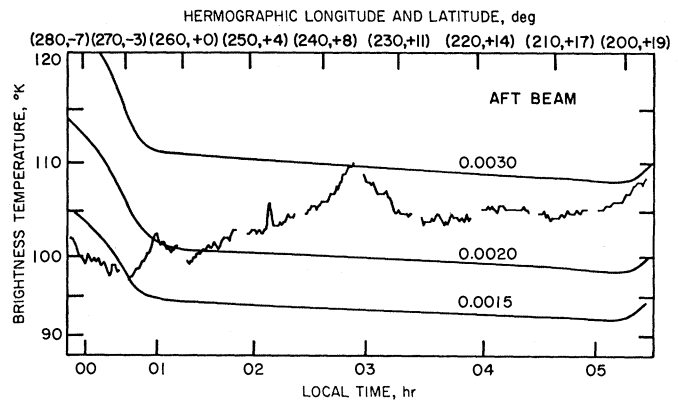


Fig. 2 (bottom). Same as Fig. 1, but for the observation with the aft beam.

received, and all coordinates given must be considered preliminary.

Figure 1 illustrates the forward beam observations from before 20 hours local time to shortly before local midnight. The plot is linear in the recorded intensity of the 45- μm radiation and in the spacecraft time, although the figure is labeled in units of brightness temperature and of hermographic (Mercurian) time and longitude. The region of precipitous decline in temperature immediately following sunset ends just before the start of the plot. The temperatures along this trace decline smoothly from 130° to 105°K, exactly as would be expected for a homogeneous material with low thermal conductivity. The predictions of three calculated homogeneous models that differ only in the thermal inertia are also illustrated (4, 5). The observed cooling curve for this part of Mercury corresponds to a thermal inertia of 0.0017 and suggests that the minimum, predawn temperature will be $\sim 90^\circ\text{K}$. Only one large thermal anomaly, with an amplitude of $\sim 3^\circ\text{K}$, is conspicuous (near longitude 290°). On the scale of the figure, instrumental noise is negligible and the small-scale structure seen in the data is real.

Figure 2 illustrates the data from the aft beam obtained between 00 and 05 hours local time and plotted on the same scale as Fig. 1. Clearly the areas of Mercury seen in this swath do not exhibit nearly as homogeneous thermal properties as those discussed in the previous paragraph. The brightness temperature reaches a minimum of about 100°K near 00 hours and then rises slowly, with superimposed fluctuations of several degrees, toward the dawn terminator. Both small-scale features (comparable to or smaller than the field of view of the radiometer) and large-scale ones (> 200 km) are evident. A comparison of the observed temperatures with the models illustrated in Fig. 2 shows that the thermal inertia along much of this trace is near 0.0025, while for the largest anomaly the inertia apparently exceeds 0.003.

The data illustrated in these two figures are raw, in the sense that they have not been corrected for possible out-of-field response of the detector or for possible directionality of emissivity of the surface. The model calculations shown in Figs. 1 and 2 have, however, been convolved with the first-order estimate of the out-of-field response which

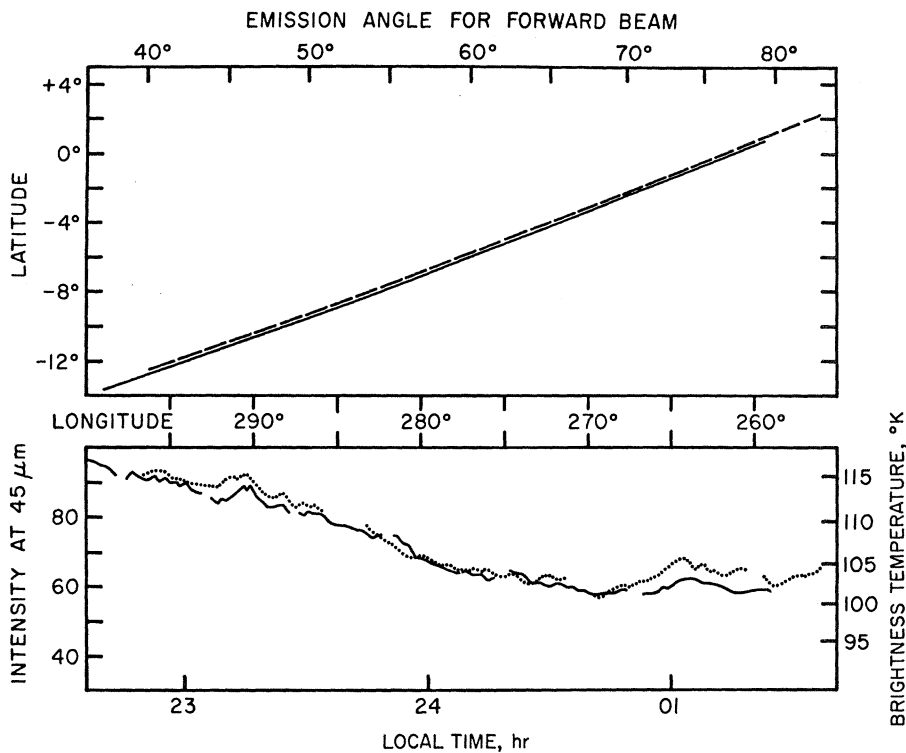


Fig. 3. Data from the region of overlap of the two beams. The upper part of the figure shows the predicted traces of the two beams. The abscissa at the top gives the emission angle as seen by the forward beam; the emission angle for the aft beam is 120° minus that of the forward beam. The temperatures have been corrected for dependence of emissivity on emission angle, as described in the text. The forward beam observations are represented by solid lines in both parts of the figure.

reproduces the onset onto the planet. The rise in temperature seen between 01 and 04 hours is thus certainly not an artifact of scattered radiation from beyond the dawn terminator of Mercury. The rise in the model temperatures of Fig. 1 for local times before ~ 20 hours is, however, an artifact of the field response; more refined fits must be made after refined trajectory data become available.

The dependence of the emissivity on direction can be investigated from the data in the region of overlap of the forward and aft beams. Figure 3 illustrates the observations made with the two beams between longitude 297° , where the emission angle into the aft beam becomes less than 80° , and longitude 258° , where the emission angle into the forward beam first exceeds 80° . The brightness temperatures from the two beams agree to within $\pm 2^\circ\text{K}$ near longitude 277° , where both view the surface at an emission angle of 60° , demonstrating the equivalence in calibration of the beams. At other places, however, the beam viewing the larger emission angles generally records the lower brightness temperature. The data from the two

beams can be brought into agreement if the measured intensity, I_ϕ is corrected according to the expression:

$$I(\phi) = I(0)\cos^\beta(\phi)$$

where ϕ is the emission angle of the infrared radiation, and the exponent $\beta = 0.2 \pm 0.01$. The observations in Fig. 3 have been corrected in this fashion, and the good agreement between the beams in general level and in many of the details of the small-scale variations is evident. Note that the linear resolutions of the two beams are similar near the start of the overlap region, but that near the end the forward beam is observing an area several times greater than that seen by the aft beam.

The thermal inertias determined from the observed brightness temperatures are characteristic of porous fragmented rock or dust similar to the lunar soil. Previous Earth-based observations have also suggested moon-like thermophysical properties for Mercury (6), but no definite measurement of any dark-side temperature has been reported. In 1923, Pettit and Nicholson (7) reported a tentative detection of thermal radiation from the night side

of the planet, suggesting a temperature of the order of 180°K , but subsequently they failed to repeat this detection (5, 8). From $10\text{-}\mu\text{m}$ scans made with the Hale 200-inch telescope several years ago, Murray (9) set an upper limit of 150°K to the mean night temperature on the planet. Murdock and Ney (10) attempted to separate the radiation emitted from the dark side from that of the illuminated part of the disk on the basis of observed color temperatures over the spectral range 3.75 to $12\ \mu\text{m}$ and concluded that the mean temperature of the night side was $111^\circ \pm 3^\circ\text{K}$. In contrast, the temperatures measured by Mariner 10 near the equator of Mercury suggest that the disk-averaged $12\text{-}\mu\text{m}$ flux from the night side should be smaller by about a factor of 2 than the amount deduced by Murdock and Ney.

There is a substantial literature on microwave radiometry of Mercury (11), in which measurements of disk-averaged temperatures originating in material tens of centimeters below the surface have been reported. The amplitudes of the variations in microwave brightness as Mercury rotates define the ratio of electrical to thermal skin depths, which has a value of 0.9 ± 0.3 at a wavelength of $1\ \text{cm}$ (6, 11). The thermal inertia of 0.002 determined from these Mariner 10 observations corresponds to a thermal skin depth of $22/\rho\ \text{cm}$, where ρ is the mean density in the upper subsurface. The electrical skin depth for microwaves is then given by $20\lambda/\rho$, where λ is the wavelength in centimeters. This quantity is, in turn, a function of dielectric constant [known from radar studies to be $\epsilon \approx 2.9$ (6)] and the electrical loss tangent. Thus, we can obtain not only the basic thermal parameter of the soil but also the basic electrical parameter, the loss tangent divided by the density. This value is $\tan\Delta/\rho = 0.005 \pm 0.001$, in excellent agreement with laboratory measurements of dry silicate rock powders (12).

The Mariner 10 radiometer observations of the night side of Mercury are consistent with the presence of a moon-like layer of insulating silicate dust constituting at least the upper tens of centimeters of the soil. The spatial variations in the thermophysical properties of this layer, as seen in these two scans across the planet, are considerable, however, suggesting large-scale regions of enhanced thermal conductivity. These could be either areas

in which the soil is more compacted or areas in which there are boulders or outcroppings of rock that are not blanketed by dust. In the absence of images of the regions of Mercury observed by the radiometer, we cannot comment on possible relationships between the thermal structure and surface morphology.

S. C. CHASE

Santa Barbara Research Center,
Goleta, California 93017

E. D. MINER

Jet Propulsion Laboratory,
California Institute of Technology,
Pasadena 91103

D. MORRISON

Institute for Astronomy, University
of Hawaii, Honolulu 96822

G. MÜNCH

G. NEUGEBAUER, M. SCHROEDER
California Institute of Technology,
Pasadena 91109

References and Notes

1. The thermal inertia is the square root of the product of the thermal conductivity (K) and the heat capacity per unit volume (ρc). In this report we express this parameter in the familiar units of $\text{cal cm}^{-2} \text{sec}^{-1/2} \text{ }^\circ\text{K}^{-1}$; these numbers can be converted to S.I. units of $\text{erg cm}^{-2} \text{sec}^{-1/2} \text{ }^\circ\text{K}^{-1}$ by multiplying by $4.2 \times 10^7 \text{ erg/cal}$.
2. S. C. Chase, *Appl. Opt.* **8**, 639 (1969).
3. The maximum temperature expected, near noon on the equator, was 560°K at the time of the Mariner 10 encounter. The substantial variations in the maximum temperatures with hermographic longitude that result from the high eccentricity of the orbit of Mercury are not expected to affect the nighttime temperatures significantly.
4. The models assume a homogeneous material with temperature-independent thermal properties and a plane-parallel geometry. The method of calculation is described by D. Morrison [*Smithson. Astrophys. Obs. Spec. Rep. No. 292* (1969) and (5)]. As shown in these references, the existence of temperature-dependent thermal properties has little effect on calculated surface temperatures.
5. D. Morrison, *Space Sci. Rev.* **11**, 271 (1970).
6. For a general review of Earth-based studies of the thermophysics of Mercury, see Morrison (5).
7. E. Pettit and S. B. Nicholson, *Publ. Astron. Soc. Pac.* **35**, 194 (1923). For additional discussion see Soter (8) and Morrison (5).
8. S. L. Soter, *Science* **153**, 1112 (1966).
9. B. C. Murray, *Trans. Am. Geophys. Union* **48**, 148 (1967).
10. T. L. Murdock and E. P. Ney, *Science* **170**, 535 (1970).
11. The ratio of skin depths is determined primarily by the observations at 3.3 mm by E. E. Epstein, M. M. Dworetzky, W. G. Fogarty, J. W. Montgomery, and R. C. Cooley [*Radio Sci.* **5**, 401 (1970)] and at 3.75 cm by M. J. Klein (*ibid.*, p. 397). More recent microwave measurements are reported in D. Morrison and M. J. Klein, *Astrophys. J.* **160**, 325 (1970); B. L. Ulich, J. R. Cogdell, J. H. Davis, *Icarus* **19**, 59 (1973); F. H. Briggs and F. D. Drake, *Astrophys. J.* **182**, 601 (1973); and J. N. Cuzzi, *ibid.*, in press.
12. M. J. Campbell and J. Ulrichs, *J. Geophys. Res.* **74**, 5867 (1969).
13. We thank the entire Mariner team, both at Jet Propulsion Laboratory and at Santa Barbara Research Center, for making the mission successful. We thank J. Bennett for help with the data analysis, J. Engel for his work as leader of the radiometry group at SBRC, and T. Clarke for his work as instrument engineer.

31 May 1974

12 JULY 1974

Observations at Mercury Encounter by the Plasma Science Experiment on Mariner 10

Abstract. A fully developed bow shock and magnetosheath were observed near Mercury, providing unambiguous evidence for a strong interaction between Mercury and the solar wind. Inside the sheath there is a distinct region analogous to the magnetosphere or magnetotail of Earth, populated by electrons with lower density and higher temperature than the electrons observed in the solar wind or magnetosheath. At the time of encounter, conditions were such that a perpendicular shock was observed on the inbound leg and a parallel shock was observed on the outbound leg of the trajectory, and energetic plasma electron events were detected upstream from the outbound shock crossing. The interaction is most likely not atmospheric, but the data clearly indicate that the obstacle to solar wind flow is magnetic, either intrinsic or induced. The particle fluxes and energy spectra showed large variations while the spacecraft was inside the magnetosphere, and these variations could be either spatial or temporal.

An unexpectedly strong interaction between the solar wind and Mercury was detected by the plasma science experiment (PSE) when Mariner 10 encountered Mercury on 29 March 1974. Before this encounter, the interaction was generally thought to resemble that of the moon, where the solar wind impinges directly on the surface. Planets, such as Earth and Jupiter, having strong magnetic fields, hold the solar wind off from the surface and deflect its flow around a cavity larger than the planet itself. Results from Mariner 5 and Mariner 10 have indicated that at Venus the solar wind is deflected by a well-developed ionosphere. Mercury presents to the solar wind an obstacle more analogous to Earth than to the moon or Venus.

This report presents preliminary results from the rearward-looking (anti-solar) electrostatic analyzer which forms

part of the plasma science experiment on Mariner 10. This experiment, a cooperative effort by groups from the Massachusetts Institute of Technology (MIT), the Los Alamos Scientific Laboratory (LASL), the Goddard Space Flight Center, and the University of California at Los Angeles, has been described previously (1) in connection with the encounter of Mariner 10 with Venus. These first measurements of plasma electrons in the vicinity of Mercury clearly show the presence of a bow shock and sheath region, resulting from deflection of the solar wind around the planet, enclosing a region which we tentatively identify as a "magnetosphere," containing a population of electrons whose properties differ from those in the surrounding medium, even though we cannot conclude whether they are trapped.

The data on which this interpretation

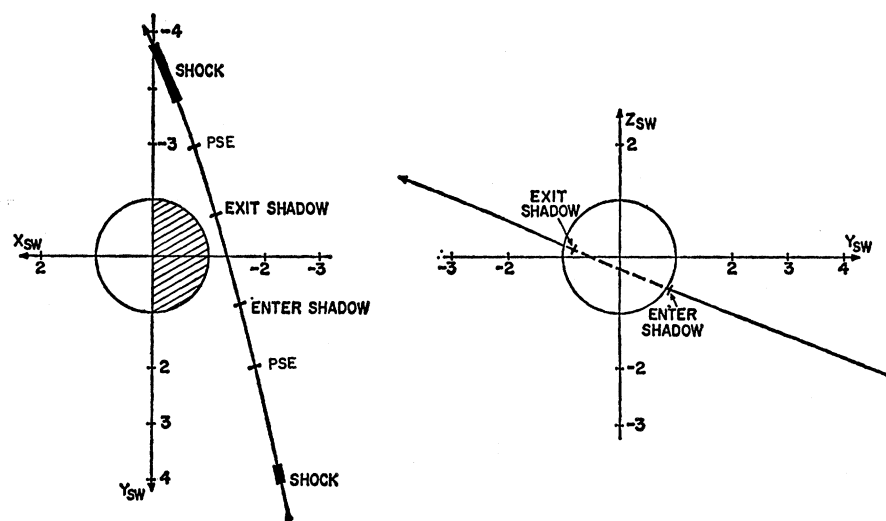


Fig. 1. The trajectory of Mariner 10 at the time of encounter with Mercury. Distances are in planetary radii, and the X_{sw} axis points in the antisolar wind direction taken to be 3° to the west of the sun. The Z_{sw} axis is to the north in the right-hand coordinate system.